Bulletin of Mathematical Biology (1998) **60**, 275–305

Testing a Model for the Dynamics of Actin Structures with Biological Parameter Values

ATHAN SPIROS AND LEAH EDELSTEIN-KESHET
Department of Mathematics,
University of British Columbia,
Vancouver, BC, V6T 1Z2, Canada
E-mail: spiros@math.ubc.ca
E-mail: keshet@math.ubc.ca

A simple mathematical model for the dynamics of network-bundle transitions in actin filaments has been previously proposed and some of its mathematical properties have been described. Other models in this class have since been considered and investigated mathematically. In this paper, we have made the first steps in connecting parameters in the model with biologically measurable quantities such as published values of rate constants for filament–crosslinker association. We describe how this connection was made, and give some preliminary numerical simulation results for the behavior of the model under biologically realistic parameter regimes. A key result is that filament length influences the bundle-network transition.

1. INTRODUCTION

Actin filaments are an essential part of the cytoskeleton, the cohesive meshwork of filaments inside the cell responsible for internal movements of fluids, particles and organelles (Parfenov *et al*., 1995; Giuliano and Taylor, 1995) as well as for the shape and movement of the cell itself (Bray, 1992; Janmey *et al*., 1994; Luby–Phelps, 1994; Wachsstock *et al*., 1993, 1994; Zaner, 1995). Microtubules, intermediate filaments, and actin filaments together form the cytoskeleton. For a good review, the reader should consult Alberts *et al*. (1989).

Actin filaments (F-actin) are formed from actin monomers (G-actin) whose molecular weight is 42 kDa: 370 monomers make a filament 1 micron (1 μ) in length with a diameter of 7–8 nm. For lengths commonly found *in vivo*, between 0.1 and 1 μ, the filaments behave like rigid rods (Janmey *et al*., 1986). Actin has been found in every plant and animal cell studied. As part of the cytoskeleton, actin filaments are involved in cell movements such as phagocytosis, cytokinesis (cell division), cell crawling, and muscle contraction. They also give the cell structure and mechanical stability. To accomplish all this, the cytoplasm contains actin in a variety of forms: linear bundles, orthogonal networks, and gels (Otto, 1994). How transitions take place between these structures is the main question which models for actin dynamics (cited above) have addressed.

0092-8240/98/020275 + 31 $25.00/0 bu970022

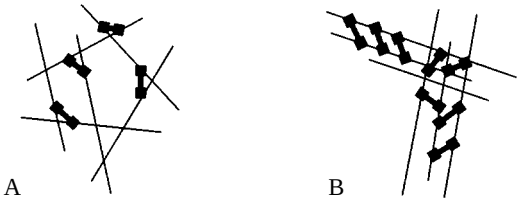

Figure 1. The transition between networks and bundles is known to occur *in vitro* as the concentration of α-actinin increases from low A to high B values. After (Wachsstock *et al*., 1993). A theoretical model for actin dynamics should be able to account for such observations.

A typical transition seen *in vitro*, shown in Fig. 1, is discussed in the experimental literature. This figure shows the effect of increasing the concentration of a crosslinker called α-actinin. The actin filaments switch between a loose meshwork in which filaments are randomly oriented, and a tight set of bundles, in which alignment is parallel. A variety of actin-binding proteins are known to cause binding of actin filaments at various configurations (Otto, 1994; Hartwig and Kwiatkowski, 1991). More information about the properties, sizes, functions, and effects of these proteins is emerging continually (Colombo *et al*., 1993; Meyer and Aebi, 1990; Maciver *et al*., 1991; Taylor and Taylor, 1994; Jockusch and Isenberg, 1981; Burridge and Feramisco, 1981). A summary of some of the more prominent players and their relative sizes is given in Alberts *et al*. (1989). We have chosen to use the crosslinker α-actinin as a particular case study for this investigation, because much of its kinetic and chemical properties are known. Our main aim is to show that such transitions can occur in models for actin dynamics with appropriate biological values.

2. GLOSSARY OF PARAMETERS

x	Spatial position
θ	Orientation
L	Average length of an actin filament
d	Diameter of an actin filament
$N(x,\theta,t)$	Number density of network (i.e. bound) filaments at x,θ
$F(x,\theta,t)$	Number density of free filaments at x,θ
$\mathcal{F}$	Total concentration of actin (in all forms) in μM
μ_1	Rotational diffusion coefficient for actin filaments
μ_2	Translational diffusion coefficient for actin filaments
β_1	Effective binding rate for two free actin filaments via binding protein
β_2	Effective binding rate for free and network filaments via binding protein

γ	Effective unbinding rate for network filaments
$K_1(\theta)$	Angular dependence of the binding rate
$K_2(x)$	Spatial dependence of the binding rate
σ_1	Angular range of interaction of filaments for binding by crosslinker
σ_2	Spatial range of interaction of filaments for binding by crosslinker
$\mathcal{A}$	Total concentration of crosslinker such as α-actinin (in both bound and free forms)
$[\alpha]$	Concentration of unbound crosslinker
k_+	Association rate constant for cross-linker and actin
k_-	Dissociation rate constant for cross-linker and actin
$D_{\Omega 0}$	Rotational diffusion coefficient of rod-like polymer in dilute solution
D_Ω	Rotational diffusion coefficient of rod-like polymer in semi-dilute solution
D_S	Translational diffusion coefficient of rod-like polymer in semi-dilute solution
ν	Total actin filament number concentration (number of filaments per unit volume)
η_s	Solvent viscosity
k_bT	Boltzmann's constant multiplied by temperature in K

3. Summary of the Model

A model related to the following was first proposed as a system for describing the parallel alignment of whole cells by Edelstein-Keshet and Ermentrout (1990). It was then adapted to the case of actin structures by Civelekoglu and Edelstein-Keshet (1994), and then developed and analyzed further in the spatially heterogeneous case by Mogilner and Edelstein-Keshet (1996). For this reason, we keep the model development relatively brief. The reader should consult the original papers for more details. This is one model in a set of possible filament-binding models whose relevance we chose to investigate. A comparison with other models for filament associations is also under investigation.

A central feature of the model is the hypothesis that actin filaments interact not merely at a single point, but rather over some spatial and angular extent. The kernel function which appears in convolutions below, represents the probability that two filaments at relative angle θ and 'center-of mass-distance' x will interact, attract, align, and bind to each other, and this in turn, depends on the types of binding proteins that are present. Actin filament interactions were modeled with the following set of integral partial differential equations for free (F) and network (N) filament density:

$$N_t(x,\theta,t) = \underbrace{\beta_1 F K * F + \beta_2 N K * F}_{\text{filament association}} \quad \underbrace{-\gamma N}_{\text{filament dissociation}}$$

$$F_t(x,\theta,t) = \overbrace{-\beta_1 F K * F - \beta_2 F K * N}^{\text{filament association}} \quad \overbrace{+\gamma N}^{\text{filament dissociation}} \quad \overbrace{+\mu_1 F_{\theta\theta}}^{\text{rotational diffusion}} \quad \overbrace{+\mu_2 F_{xx}}^{\text{translational diffusion}}.$$

The assumptions incorporated into the model are that the average length of the filament, L is fixed, and that free filaments may diffuse rotationally, μ_1, and translationally, μ_2. Unbinding of filaments from the network is assumed to take place at rate γ. Binding of filaments (convolution terms) is assumed to occur at a rate that depends on relative configurations $K * F$ where

$$K * F = \int_{-\pi}^{\pi} \int_{\Omega} K(\theta - \theta', x - x') F(x', \theta') d\theta' dx' . \tag{1}$$

This makes such models nonlocal in that filaments can interact over some spatial and angular ranges. The kernels (K) considered in some of the previous models of actin dynamics have typically had the form

$$K(\theta, x) = K_1(\theta) K_2(x), \tag{2}$$

where

$$K_i(u) = \frac{1}{\sigma_i \sqrt{2\pi}} \exp\left(-\frac{u^2}{2\sigma_i^2}\right). \tag{3}$$

K_1 describes the angular part of the way filaments interact in the presence of a crosslinker, and K_2 the spatial part. The parameter σ_1 is the angular range over which filaments can interact and σ_2 is the spatial range. The kernel $K(\theta, x)$ can be adapted to a variety of cases, including interactions that tend to create parallel or orthogonal configurations, that tend to bunch filaments together, etc. (Civelekoglu and Edelstein-Keshet, 1994).

This model has a number of limitations to be recognized, among which are:

(i) The model does not take into account possible filament length changes due to polymerization or fragmentation. The average filament length L is assumed to be constant in a given situation. However, the effect of this parameter on the types of structures that form will be a theme in the paper. For a recent review of how changes in filament length can be modelled, see Edelstein-Keshet and Ermentrout (1997) and Ermentrout and Edelstein-Keshet (1997).

(ii) This simple continuum model does not discriminate between various binding states of a given filament. Only two binding states are represented: bound and free filaments. This means that:

- a filament bound at the edge of the cluster is treated in the same way as one bound inside the cluster;
- a filament bound by one crosslinker is treated in the same way as a filament bound by multiple crosslinkers.

(iii) The diffusion rate of filaments is not assumed to depend explicitly on the local density surrounding the filament. Thus, a free filament that happens to penetrate the network is not assumed to have a lower rate of diffusion. (However, the probablility that it binds, and thus stops moving is increased.)

(iv) The model does not incorporate any mechanical or fluid dynamic effects (membranes, cytoplasmic streaming, effects of organelles) nor interactions with myriad ions, proteins, motors, etc. in the cell. It is thus mainly relevant to *in vitro* actin dynamics.

The above limitations are partly attributable to the fact that a continuum model necessarily averages over the fine details of the discrete physical system, and partly due to simplifying assumptions that could be lifted in more detailed versions of such a model.

The dimensionless formulation of the model equations and properties of its uniform steady-state solution, $\bar{F}, \bar{N}$ are described briefly in the Appendix for completeness. The aspect of interest to formation of alignment patterns is the fact that the uniform situation, $\bar{F}, \bar{N}$ (in which actin filaments are distributed uniformly over space and are isotropic—i.e., have no inherent directionality) can be disrupted. The occurrence of this effect can be probed by linear stability analysis of the equations. *The homogeneous steady state, $\bar{F}, \bar{N}$ is destabilized whenever the following condition is satisfied:*

$$\mu_1 k_1^2 + \mu_2 k_2^2 < \left(\frac{\beta_1 \beta_2}{\gamma}\right) \tilde{M}^2 \hat{K} \left(1 - \hat{K}\right) \tag{4}$$

where $\tilde{M} = \bar{F} + (\beta_2/\beta_1)\bar{N}$. The wavenumbers, k_1, k_2 correspond, respectively, to the angular and spatial parts of the deviations (from steady state) that cause destabilization (Civelekoglu and Edelstein-Keshet, 1994). $\hat{K} = \hat{K}(k_1, k_2)$ is the spatio-angular Fourier transform of the kernel K, and is a function of the wavenumbers. For example, in the case of the kernel suggested in equation (3),

$$\hat{K} = \exp\left[\frac{-1}{2}\left(\sigma_1^2 k_1^2 + \sigma_2^2 k_2^2\right)\right]. \tag{5}$$

The condition given by the inequality (4) is necessary for small perturbations to grow. As such, it can suggest regimes of interest to be explored numerically. However, how these perturbations develop further depends on nonlinear interactions in the model. The role of simulations is to reveal how these combined effects produce overall patterns. Partial analysis of these equations

suggests intriguing pattern formation and bifurcations (Mogilner and Edelstein-Keshet, 1996). Treatment of similar models analytically Geigant *et al*. (1997) and with advanced numerical methods has also been undertaken by Geigant and Stoll (1996). However, a full numerical analysis of the above equations with realistic parameter values has not yet been carried out. The main thrust of this paper is the investigation of the extent to which the biological literature can be used to estimate a full set of parameter values for the model, and the resulting analysis and interpretation of numerical simulations, as well as an emphasis on the influence of filament length on the structures that form.

4. Estimation of Parameter Values

The model parameters are not explicitly given in the literature, but must be deduced from the basic processes that are assumed. Parameter estimation is challenging because one parameter in the model describes the effects of several processes. Careful consideration of the underlying chemical and physical processes is needed to relate the known biological quantities to the model parameters. This is the main theme developed in the next few sections. The values of some of the model parameters will be based on the rate constants for the crosslinker binding to actin filaments. Typical values for α-actinin on which we concentrate in this paper are given in Table 1. The results can be extended to other crosslinkers in a straightforward way.

Table 1. Association–dissociation rate constants for α-actinin cross-linker and actin.

Parameter	Value	Source
k_+	1 μM^{-1} s^{-1}	Chicken smooth-muscle α-actinin (Wachsstock *et al*., 1994)
	1 μM^{-1} s^{-1}	*Acanthamoeba* α-actinin
k_-	0.67 s^{-1}	Chicken smooth-muscle α-actinin
k_-	5.2 s^{-1}	*Acanthamoeba* α-actinin
k_-	3 s^{-1}	'Generic' (Lumsden and Dufort, 1993)
k_+	3 μM^{-1} s^{-1}	
$K_d = k_-/k_+$	0.4 μM	Chicken gizzard α-actinin 22 °C (Meyer and Aebi, 1990)
	2.7 μM	*Acanthamoeba*
	2.7 μM	*Dictyostelium*

4.1. ***Estimating the filament association rate, β_i.*** The parameters β_i represent the rate of filament association through the influence of crosslinkers: β_1 is the

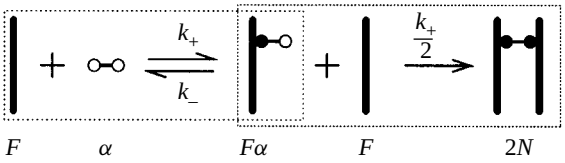

Figure 2. Two free filaments must first interact with an α-actinin before they can bind to one another. The rate of the first reaction is well known from the literature (Wachsstock *et al*., 1994). The rate of the second reaction is deduced from the fact that only one actin-binding domain (as opposed to the two actin-binding domains available for free α-actinin) can bind with the filament.

rate that two free filaments bind to form two network filaments, and β_2 the rate that a free filament binds to part of the network. In the simplest case, one of the binding domains of a crosslinker such as α-actinin attaches to an actin filament and then the second binding domain adheres to a neighboring filament resulting in a filament–filament association (see Fig. 2).

The process shown in Fig. 2 represents the binding steps involved in creating network filaments, and leads to the estimate for β_i. The association–dissociation rate constants of α-actinin and actin, k_+ and k_- respectively, are used in estimates of β_1 (see Table 1).

The first step of the above set of reactions can be represented by the differential equation,

$$\frac{d[\alpha]}{dt} = k_+[F][\alpha] - k_-[F\alpha]. \tag{6}$$

If this reaction is rapid on the time scale of the other processes, we can assume that the concentrations $[F\alpha]$ and $[F]$ are at quasi-steady state so that we have roughly,

$$[F\alpha] = \frac{k_+}{k_-}[\alpha][F]\,. \tag{7}$$

The second reaction step in Fig. 2 leads to the binding of two filaments which are then counted as two network filaments. Thus:

$$\frac{d[N]}{dt} = 2\frac{k_+}{2}[F\alpha][F]\,. \tag{8}$$

Substituting the quasi-steady state value of $[F\alpha]$ into this expression leads to:

$$\frac{d[N]}{dt} = k_+\frac{k_+}{k_-}[\alpha][F][F] = \left(\frac{k_+^2[\alpha]}{k_-}\right)[F]^2\,. \tag{9}$$

The coefficient in front of the F^2 term is then the estimate for β_1, i.e.,

$$\beta_1 \approx \left(\frac{k_+^2[\alpha]}{k_-}\right)\,. \tag{10}$$

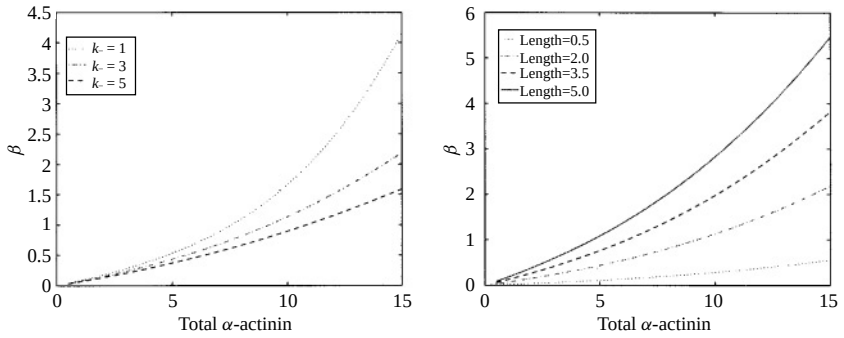

Figure 3. The figure on the left shows how the cross-linker dissociation rate, k_-, affects β_1 as a function of $\mathcal{A}$. The figure on the right shows how filament length, L affects β_1. The amount of actin is fixed at 15 μM.

This estimate for β_1 is given in terms of free α-actinin concentration. We can relate this (generally unknown) parameter to the total amount of α-actinin, $\mathcal{A}$, and the total amount of actin $\mathcal{F}$ as follows: Wachsstock *et al*. (1993) determines the equilibrium dissociation constant for α-actinin, $K_d = k_-/k_+$ and notes that

$$\frac{\text{bound } \alpha\text{-actinin}}{\text{total actin}} = \frac{\text{free } \alpha\text{-actinin}}{K_d + \text{free } \alpha\text{-actinin}} \tag{11}$$

or in terms of our parameters

$$\frac{\mathcal{A} - [\alpha]}{\mathcal{F}} = \frac{[\alpha]}{K_d + [\alpha]}\,. \tag{12}$$

Solving for $[\alpha]$ in the above equation yields

$$[\alpha] = \tfrac{1}{2}\left[(\mathcal{A} - \mathcal{F} - K_d) + \sqrt{(\mathcal{A} - \mathcal{F} - K_d)^2 - 4\mathcal{A}K_d}\right]. \tag{13}$$

We can substitute this value into the expression for β_1 given by equation (10) to express the estimate in terms of the total amount of α-actinin. To apply these results to actual (numerical) parameter values, units conventionally used in rate constants and concentrations (μM) must be converted to units appropriate for the variables used here, namely *number of filaments per unit volume*. This involves some detailed conversions which are described in the Appendix. Typically, for $k_+ = 1\ \mu\text{M}^{-1}\ \text{s}^{-1}$, we find that β_1 (in units of per filament density per second) is

$$\beta_1 \approx \frac{0.61L[\alpha]}{k_-}. \tag{14}$$

The factor of 0.61 converts the μM units for $[\alpha]$ and the μm units for the filament length L to units appropriate for β_1 (see Appendix).

All three of the main biological parameters (the filament length, L, the total concentration of α-actinin, $\mathcal{A}$, and the crosslinker dissociation rate, k_-) influence

β_1. Fig. 3 shows how several values of k_- and L affect β_1 as a function of $\mathcal{A}$. If the first reaction shown in Fig. 2 is not rapid, then our estimate for β_1 is too high. If, on average, a filament has many crosslinkers attached to it, then our estimate for β_1 is too low.

When a free filament binds to a network filament, only *one* new network filament is formed. Thus, an estimate for β_2 might be $\beta_2 \approx \beta_1/2$. However, a reviewer of this paper noted that a second-order reaction rate depends on the sum of the diffusion rates of its reactants, and since one of the filaments was initially bound, it may be more accurate to set $\beta_2 \approx \beta_1/4$. We ran simulations where β_2 was $\beta_1/2$ and compared these results with simulations where β_2 was $\beta_1/4$. There were some changes in the amount of clustering at short lengths but the final outcome for most simulations changed very little.

4.2. ***Estimating the rate of filament-network dissociation, γ.*** The model equations include a term for the dissociation of filaments from the network, γ. Recall that the model is not meant to distinguish individual filaments with many crosslinks from those with few crosslinks, nor filaments surrounded by other filaments from those that are relatively isolated. The estimate of γ averages these individual properties, to come up with one aggregate 'average' unbinding rate parameter. To estimate this rate, we consider the steps that lead a filament to be liberated when it is initially bound to the network, a process which takes many steps. Depending on assumptions made, there are several ways of estimating the *aggregate* parameter that reflects the overall rate. An upper bound for γ is k_- (in the unrealistic limit that each filament is linked to the network by a single crosslink, the rate of dissociation of a filament would be simply the rate of dissociation of a single crosslinker, which is just k_-). Since, on average, network filaments have two or more crosslinks, the true dissociation rate of a filament from the network is slower than k_-.

We estimate γ by studying the set of chemical steps that lead to a single-filament dissociation. Let x_i denote a network filament with i attached α-actinin crosslinkers. We must consider the simultaneous association–dissociation steps that can occur: a crosslinker can bind or unbind from the filament. Thus x_i can be converted to x_{i+1} (at the rate $[\alpha]k_+$, i.e., depending on the availability of free crosslinkers) and x_i goes to x_{i-1} (at the rate ik_- which depends only on the number of attached α-actinin). If up to n α-actinin can bind to a filament, then the entire process is described by the following reactions

$$x_n \underset{[\alpha]k_+}{\overset{nk_-}{\rightleftharpoons}} x_{n-1} \underset{[\alpha]k_+}{\overset{(n-1)k_-}{\rightleftharpoons}} x_{n-2} \underset{[\alpha]k_+}{\overset{(n-2)k_-}{\rightleftharpoons}} \cdots \underset{[\alpha]k_+}{\overset{(i+1)k_-}{\rightleftharpoons}} x_i \underset{[\alpha]k_+}{\overset{ik_-}{\rightleftharpoons}}$$

$$\cdots \underset{[\alpha]k_+}{\overset{4k_-}{\rightleftharpoons}} x_3 \underset{[\alpha]k_+}{\overset{3k_-}{\rightleftharpoons}} x_2 \underset{[\alpha]k_+}{\overset{2k_-}{\rightleftharpoons}} x_1 \overset{k_-}{\rightarrow}.$$

Since the above system is more intricate than the one used for estimating β, it calls for a different analysis. Essentially, our approach is to ask how quickly, on average, a filament can move through the above sequence of steps. To answer this question, we represent the chemical kinetics with a system of ordinary differential equations for the x_is given below. The system is linear if we assume that the level of free crosslinkers is held fixed (Jacquez, 1972):

$$\begin{aligned}
\frac{d[x_n]}{dt} &= -nk_-[x_n] + [\alpha]k_+[x_{n-1}], \\
\frac{d[x_i]}{dt} &= (i+1)k_-[x_{i+1}] - ([\alpha]k_+ + ik_-)\,[x_i] + [\alpha]k_+[x_{i-1}] \qquad (15) \\
&\quad \text{for } n-1 \geq i \geq 2, \\
\frac{d[x_1]}{dt} &= -([\alpha]k_+ + k_-)\,[x_1].
\end{aligned}$$

Note that the longer the filament, the greater the number of possible binding sites for a crosslinker: hence coefficients in the above system depend on the size i of the given filament. We will assume that the maximal number of crosslinks that can bind to a filament is n, so that the above is a system of n linear differential equations. The equations are in $n \times n$ tridiagonal form so that their corresponding matrix is,

$$\begin{bmatrix}
-([\alpha]k_+ + k_-) & 2k_- & 0 & 0 & \dots & 0 & 0 & 0 \\
[\alpha]k_+ & -([\alpha]k_+ + 2k_-) & 3k_- & 0 & \dots & 0 & 0 & 0 \\
0 & [\alpha]k_+ & -([\alpha]k_+ + 3k_-) & 4k_- & \dots & \vdots & \vdots & \vdots \\
\vdots & \vdots & \vdots & \vdots & \dots & [\alpha]k_+ & -([\alpha]k_+ + (n-1)k_-) & nk_- \\
0 & 0 & 0 & 0 & \dots & 0 & [\alpha]k_+ & -nk_-
\end{bmatrix}.$$

The eigenvalues of this matrix describe the 'rates of flow' through the system. If all the eigenvalues are negative, an initial group of network filaments will eventually disappear from the system as they are liberated, one by one. In this case, the negative eigenvalue of smallest magnitude, λ_m, represents the 'rate limiting' decay, i.e the slowest rate of decay in the system, which we take to be an estimate for $-\gamma$.

The estimate for γ might seem to be sensitive to the assumed maximal crosslinker occupancy level, n. However, as shown by Fig. 4, γ reaches a limit as n increases (while other parameters are held fixed). Our task is now reduced to

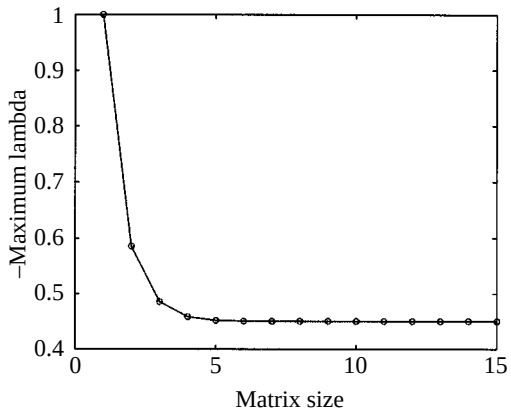

Figure 4. The negative eigenvalue of smallest magnitude, $-\lambda_m$, reaches a limit as the maximal number of crosslinks, n, and thus the size of the $n \times n$ matrix increases. The biological parameters for this figure have been fixed at $[\alpha] = 1$ μM, $k_+ = 1$ μM^{-1} s^{-1} and $k_- = 1$ s^{-1}. γ (in units of s^{-1}) does not change significantly after $n = 5$ in this case.

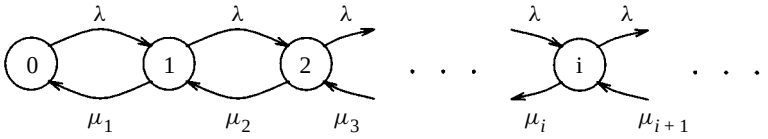

Figure 5. The number of cross-linkers attached to a filament can be viewed as a birth–death process. Each circle represents one 'state' of the filament (i.e. how many cross-linkers are attached). The rate of cross-linker attachment is independent of the number already attached. Thus the birth rate, $\lambda = [\alpha]k_+$, is the same for all states. The death rate, μ_i depends on the number attached to the filament: since any single one can unbind at the rate k_-, the rate that state i goes to $i-1$ is $\mu_i = ik_-$. For mathematical tractability, the time between states is assumed to be exponentially distributed with means $1/\lambda$ and $1/\mu$.

finding a suitable n, and then computing the eigenvalues of the $n \times n$ matrix. One way of deciding on an appropriate value for n is to consider the process of α-actinin binding and unbinding to be a continuous-time Markov chain (see Fig. 5). The steady-state probability, P_i, that a filament will have i α-actinin attached to it at any time is then

$$P_i = \frac{r^i}{i!}e^{-r} \qquad \text{where } r = \frac{[\alpha]k_+}{k_-}. \tag{16}$$

n can then be determined by placing a bound on the likelihood of a state existing. Suppose a steady-state probability less than 0.1% is insignificant. Then n is the maximum i such that $P_i \geq 0.001$ (e.g. if $[\alpha] = 1$, $k_+ = 1$, and $k_- = 1$, then $n = 5$ because $P_5 = 0.003$, but $P_6 = 0.0005$).

We can now find γ with a simple algorithm. First, take the biological parameter values and calculate n. Next calculate the eigenvalues from the resulting $n \times n$ matrix and take $\gamma \approx -\lambda_m$ where λ_m is the negative eigenvalue of smallest

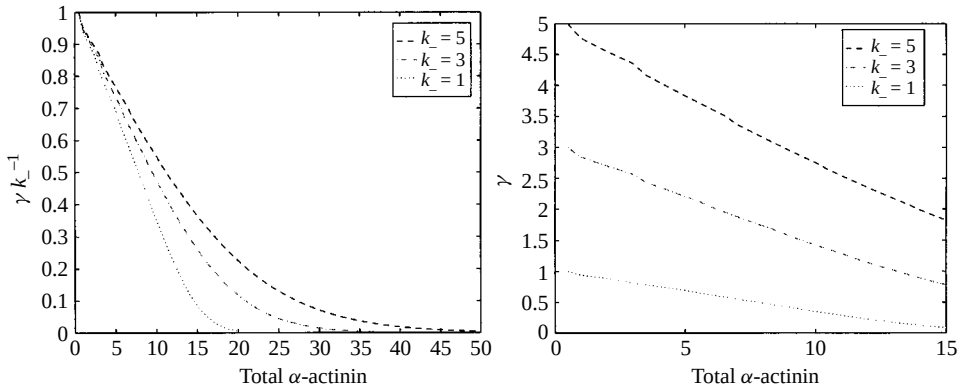

Figure 6. The dependence of γ on total available α-actinin, A (in units of μM). The figure on the left shows that γ (in units of s^{-1}) goes to zero as the amount of α-actinin is increased. The figure on the right shows that γ changes linearly with respect to the total concentration of α-actinin, $\mathcal{A}$, when $\mathcal{A}$ is in the range of levels used in experimental situations (Wachsstock *et al.*, 1993). $k_+ = 1\ \mu M^{-1}\ s^{-1}$ and $\mathcal{F} = 15\ \mu$M in these graphs.

magnitude. The computer package, *Matlab*, is able to compute γ quickly with this algorithm. The results are summarized in Fig. 6.

4.3. ***Estimating filament rates of diffusion.*** Estimates of filament rates of diffusion are given in the polymer literature (Doi and Edwards, 1986). Both rotational and translational motions of filaments are important, as the filaments are being redistributed in space and over various orientations (in bundles and gels). The translational and rotational rates of diffusion of filaments depend on filament lengths in distinct ways. Entanglement occurs in the regime of *semidilute* behavior. This effect is felt when the number of filaments per unit volume, ν, exceeds $(\pi/6)L^3$, where L is filament length. For example, at a typical *in vitro* actin concentration of 1 mg/ml, semi-dilute behavior occurs beyond a length of 0.225 μ, the length of a filament consisting of roughly 84 actin monomers (Zaner, 1995). At 15 μM the lengths for the semi-dilute regime are $0.2\ \mu < L < 5.5\ \mu$ while at 100 μM, a concentration more typical of the *in vivo* conditions, the lengths for the semidilute regime are $0.08\ \mu < L < 0.82\ \mu$. (This implies that in the *in vivo* case, steric interactions of filaments which are a few monomers long will play a dominant role.) Since the model assumes that the filaments are able to diffuse readily, it is more suitable for describing the lower concentrations typical of the *in vitro*, rather than the higher concentrations of the *in vivo*, cases.

In a *dilute solution*, the *Rotational Diffusion Coefficient*, $D_{\Omega 0}$, is (Doi and Edwards, 1986):

$$D_{\Omega 0} = \frac{3k_bT\ln(L/d - b)}{\pi\eta_s L^3} \tag{17}$$

where L is the length of the polymer, d its diameter, k_b is Boltzmann's constant, T temperature (K), and η_s the viscosity of the solution. (b is a 'generic', empirically

determined constant, as is B in the next equation.) In a *semi-dilute solution*, the *Rotational Diffusion Coefficient*, D_Ω is (Doi and Edwards, 1986):

$$D_\Omega = \frac{B D_{\Omega 0}}{\left(\nu L^3\right)^2} . \tag{18}$$

If we consider a given, fixed, concentration of actin, say $\mathcal{F}$, and note that the number of filaments per unit volume is $\nu = \mathcal{F}/L$, we find that

$$D_\Omega = B \frac{3 k_b T \ln(L/d - b)}{\pi \eta_s} \frac{1}{\mathcal{F}^2 L^7} . \tag{19}$$

Thus, rotational diffusion in a semidilute solution falls off as the seventh power of the filament length.

The *Translational Diffusion Coefficient* is (Doi and Edwards, 1986):

$$D_S = \frac{k_b T \ln(L/d - b)}{3\pi \eta_s L} . \tag{20}$$

We can identify the diffusion parameters in the model in the following way: $\mu_1 = D_{\Omega 0}$ (in dilute solution), $\mu_1 = D_\Omega$ (in semi-dilute solution), and $\mu_2 = D_S$ in either type of solution. A summary of the parameters in these expressions and typical values is given in Table 4.3. Typical translational and rotational diffusion rates for an actin monomer in water are 90 μ^2 s^{-1} and 1.1×10^7 rad^2 s^{-1} respectively. By comparison, the rate of translational diffusion of an actin filament whose length is 1 μ in water is 2.1 μ^2 s^{-1} and the rate of rotational diffusion is 41 rad^2 s^{-1}.

Table 2. Parameter values for the diffusivities. Note that 1 erg = 1 gm cm^2 s^{-2}, 1 Poise = 1 gm cm^{-1} s^{-1}.

Parameter	Meaning	Value	Source
		0.1–1 μ	*In vivo*
L	Filament length	4.9 μ	Wachsstock (1993) *in vitro*
d	Filament diameter	7.0 nm	Lumsden (1993)
		8.0 nm	Wachsstock (1993)
		0.01 Poise	Wachsstock (1993), (water)
η_s	Solvent viscosity	0.55 Poise	Lumsden (1993)
		100–1000 Poise	Oster (cytoplasm)
k_b	Boltzmann's constant	1.38×10^{-16} ergs per degree	
T	Absolute temperature	300 K	Room temperature
B	Generic factor	1.3×10^3	Doi and Edwards (1986)
b	Generic factor	0.8	Doi and Edwards (1986)

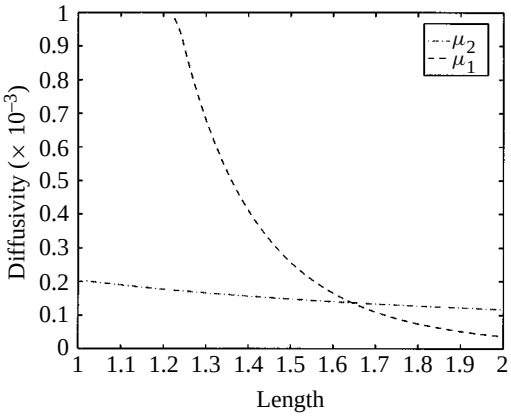

Figure 7. Diffusion rates for translational and rotational diffusion of filaments in the semi-dilute regime, as a function of filament length. Units are μ^2 s^{-1} for the translational diffusion, and radians^2 s^{-1} for the rotational diffusion. The viscosity was 100 P. The actin concentration was 15 μM.

5. Spatial and Angular Ranges of Interaction

We could find no precedent for the kernels chosen for the model, and none have as yet been measured directly. However, the behavior of the model depends on basic types of kernels used (if not their detailed shapes), and we had to supplement biological knowledge with reasonable assumptions about how filaments and binding proteins interact. For example, we assumed that:

(1) the closer the filaments, the greater the probability that they interact in the presence of a crosslinker;
(2) the more flexible (or 'floppy') the crosslinker, the greater the *angular range* of interaction;
(3) the longer the filaments, the greater their spatial range of interaction.

For a crosslinker such as chicken α-actinin, the more nearly parallel or antiparallel the filaments, the greater the probability of binding (Meyer and Aebi, 1990). Thus, in the case of chicken α-actinin, the angular part of the kernel should have maxima at $\theta = 0, \pm\pi$. For a crosslinker such as actin-binding protein (ABP), (not explicitly considered in this paper), the orthogonal configuration of filaments is favored[†] (Gorlin *et al.*, 1990; Hartwig *et al.*, 1980). Possibly, more information about detailed geometric configurations in the interactions of an actin filament with a crosslinker will become available through structural studies now being carried out by some groups (McGough, 1997).

For the spatial part of the kernel we chose a Gaussian dependence with a maximum at $x = 0$, and a width on the order of the filament length. The *Spatial Range of the Kernel*, σ_2 is related to the length of the filaments as follows. Recall

[†]See Civelekoglu and Edelstein-Keshet (1994) for further discussion of kernels appropriate to a variety of crosslinkers

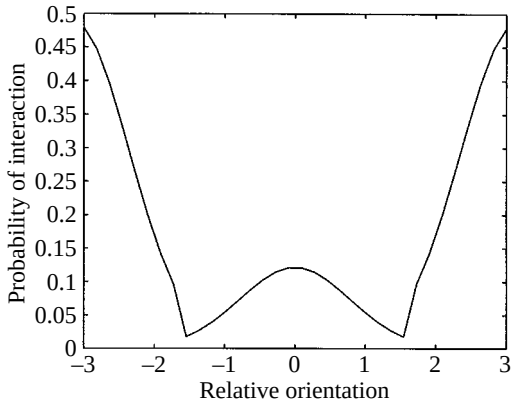

Figure 8. The form of the kernel that we chose to reflect properties of the crosslinker chicken α-actinin, which favors antiparallel alignment (Meyer and Aebi, 1990). The intensity of interactions between two filaments subtending angles between $-\pi$ and π radians are shown here.

that 68% of a Gaussian distribution is within one standard deviation of the mean and that 95% is within two standard deviations. If at least 95% of all interactions between a given filament and its neighbors take place within half a filament length distance from its center of mass, then $2\sigma_2 = L$ or

$$\sigma_2 \approx \frac{L}{2}. \tag{21}$$

The *Angular Range of the Kernel,* σ_1 is more difficult to estimate and depends on such properties as flexibility of the crosslinker. We examined what is known for a variety of proteins, including ABP. Filaments are bound by ABP at nearly 90° angles, with a distribution that appears to have a standard deviation of roughly 25° in freeze-dried, electron microscopic preparations (Niederman *et al.*, 1983). There is not, at present, a similar set of observations for α-actinin. A recent paper by Janson and Taylor (1994) also gives valuable hints about the relative sizes and bending of ABP (filamin) and α-actinin. Their work suggests that an α-actinin can 'bend' as far as 45°. Two filaments bound to this crosslinker could thus subtend angles anywhere in the range $0 < \theta < 90^\circ$. Therefore, $2\sigma_1 = \pi/2$ or

$$\sigma_1 \approx \frac{\pi}{4}. \tag{22}$$

A Gaussian centered at zero, with the above value of the angular width would be a good approximation for the kernel if the crosslinker promoted predominantly parallel alignment as in the case of *Acanthamoeba* α-actinin. However, for a crosslinker such as chicken α-actinin, which is known to favor antiparallel alignment (Meyer and Aebi, 1990), we correct the form of the kernel to incorporate this feature.

Figure 8 illustrates the angular part of the kernel we chose to model the antiparallel types of α-actinin crosslinker. The relative heights of the humps of this kernel (at $\theta = 0, \theta = \pm\pi$) were based on the relative frequency of parallel and antiparallel alignment observed experimentally using chicken α-actinin *in vitro* (Meyer and Aebi, 1990). A roughly four to one ratio of antiparallel to parallel alignment was assumed. The kernel was composed of two Gaussian shapes with σ_1 as above. The peaks were centered at $0, \pm\pi$, and each was effective over a range of π. The kernel chosen to model the parallel types of α-actinin crosslinker were the same with only the weights reversed.

6. SUMMARY OF PARAMETER VALUES

Table 3. Parameter values in units consistent with the model.

Parameter	Meaning	Value
ν	Filament concentration	$(24.4/L)$ filaments per μ^3
$[\alpha]$	Crosslinker concentration	0–3 $\times 10^3$ dimers per μ^3
k_+	For actin	$0.61 \times L$ per filament of length L μ^3 s^{-1}
	For α-actinin	3.3×10^{-3} per crosslinker μ^3 s^{-1}
k_-	Reverse rate constant	0.67–5.2 s^{-1}
L	Filament length *in vivo*	0.1–1 μ
	Filament length *in vitro*	4–6 μ
d	Filament diameter	7.5×10^{-3} μ
k_bT/η_s	In water	4.14 μ^3 s^{-1}
	In actin solution	0.075 μ^3 s^{-1}
	In cytoplasm	$4.14\times \times 10^{-4}$ μ^3 s^{-1}
$\mathcal{C}$	Log term for diffusion	$\ln((L/d) - b)$
$D_{\Omega 0}$	Rotational diffusion (dilute solution)	
	In water	$3.8(\mathcal{C}/L^3)$ s^{-1}
	Lumsden	$0.07(\mathcal{C}/L^3)$ s^{-1}
	Cytoplasm	$3.8 \times 10^{-4}(\mathcal{C}/L^3)$
D_Ω	Rotational diffusion (semi-dilute solution)	
	In water	$8.3(\mathcal{C}/L^7)$ s^{-1}
	Lumsden	$0.15(\mathcal{C}/L^7)$ s^{-1}
	Cytoplasm	$8.3 \times 10^{-4}(\mathcal{C}/L^7)$ s^{-1}
D_S	Translational diffusion	
	In water	$0.42(\mathcal{C}/L)$ μ^2 s^{-1}
	(Lumsden)	$7.8 \times 10^{-3}(\mathcal{C}/L)$ μ^2 s^{-1}
	Cytoplasm	$4.2 \times 10^{-5}(\mathcal{C}/L)$ μ^2 s^{-1}

Parameter values from the literature and calculations described in this paper were used to construct Table 6. A summary of some of the units, conversion factors, and other details which entered the calculations of specific values is given in the Appendix. In particular, literature values of concentrations are generally

specified as units of mass per unit volume, for example as mg ml^{-1} or as μM. (A typical actin concentration *in vitro* is 1 mg ml^{-1}.) The model is based on interactions of whole filaments, and thus keeps track of the number of filaments per unit volume. The final values of parameters, as they appear in the model simulations is given in Table 4.

Parameter	Range	Typical Value	Units	Comment
L	0–5	1	μ	- -
β_1	0–5	0.1	per filament concentration s^{-1}	Section 4.1
γ	0–5	0.9	s^{-1}	Section 4.2
μ_1	10^{-1}–10^{-5}	D_Ω	s^{-1}	Section 4.3
μ_2	10^{-1}–10^{-3}	D_S	$\mu^2 s^{-1}$	Section 4.3
σ_1	$\pi/8$–$\pi/4$	$\pi/4$	$rad^2 s^{-1}$	Section 5
σ_2	0-3	$L/2$	μ	Section 5

Table 4. The model parameters and ranges of values.

Using the values given in Table 3 we are ready to calculate the model parameter values. The results are shown in Table 4. When calculating these values we have set

$$\mathcal{A} = 1\ \mu\text{M}, \tag{23}$$

$$k_+ = 1\ \mu\text{M}^{-1}\ \text{s}^{-1}, \tag{24}$$

and

$$k_- = 1\ \text{s}^{-1}, \tag{25}$$

roughly corresponding to the case of chicken α-actinin (Wachsstock *et al.*, 1994). The filament length is systematically varied and results of the interactions are described in Section 8. For the one-dimensional model, we will consider a one-dimensional 'corridor' roughly 6 μm in length.

7. Numerical Methods and Techniques for Solving the Model Equations

Developing a numerical scheme to solve the equations of the model can be challenging. The convolutions (i.e. $K * F$) in the equations increase the complexity of some methods and are computationally intensive. The vast changes in the diffusion coefficients suggest the use of two different numerical methods. Also, since we are interested in the case where the homogeneous steady state is unstable, the numerical scheme must be designed to handle rapid growth as well. Previous simulations have been carried out by Civelekoglu and Edelstein-Keshet (1994) and Ladizhansky (1994) for similar model(s) in the space-independent case, and by Geigant and Stoll (1996) for the angular two-dimensional spatial

case. However, to our knowledge, this is the first case of simulations in which details of the biological parameter values have been included.

Computing the convolutions is the most costly step in the simulation. Imagine the (x, θ) space divided into an $n \times n$ grid. Each grid point must have associated with it the value of the convolution at that point. At the grid point (x_i, θ_j), the convolution for $K * F$ is the same as the integral

$$\int_{x_0}^{x_n} \int_{\theta_0}^{\theta_n} K\,(x_i - x, \theta_i - \theta)\, F(x, \theta) d\theta\, dx.$$

Using a simple integral approximation such as the trapezoid method to compute this integral at a single grid point, say (x_i, θ_j) would result in n^2 computations. (The value at each grid point must be used in the calculation.) Since this computation must be done for all n^2 grid points, the cost of computing the integrals for one time step is $O(n^4)$. We can improve on this 'primitive' method by taking advantage of the fact that we are computing a convolution.

Recall that the Fourier transform of a convolution, say $K * F$, is the same as the point-wise multiplication of the transforms, $\hat{K}$ and $\hat{F}$. Fourier transforms and their inverses can be efficiently computed with the fast Fourier transform (FFT) and the inverse fast Fourier transform (IFFT) at the cost of $O(n^2 \log_2 n)$ operations each. The cost of multiplying the transforms is n^2. Thus, a more efficient way of computing the convolution, $K * F$, is to take the FFT of F and K, multiply the transforms and take the IFFT of the result. Since these steps are sequential, costs are additive, so that the total cost is $O\left(n^2 \log_2 n\right)$. Even though this helps, computing the convolution is still the most computationally intensive part of the numerical solver.

Selecting a proper finite difference scheme is essential for solving the partial differential equation numerically. Big diffusion coefficients (when the filament lengths are small or the viscosity is close to that of water) require the use of an implicit method. However, small diffusion coefficients (when the filament lengths are big or the viscosity is greater than that of water) suggest the use of an explicit scheme. Further, a method with a high order of accuracy in time is needed to compute the solution for an unstable homogeneous steady state. These criteria lead to the use of a fourth-order Runge–Kutta method to solve the system of partial differential equations. Because it is explicit, this method takes some time to solve equations that have big diffusion coefficients but still solves them accurately.

The FFT for the convolutions was tested on trigonometric functions whose results could be verified analytically. The numerical scheme was tested for stability. When working on a grid with a spatial step size of DX and an angular step size of DA, the parabolic part of our equations requires our step size, DT, to satisfy

$$DT < \min\left\{\frac{DA}{2\mu_1}, \frac{DX}{2\mu_2}\right\}$$

in order for the scheme to be stable. We let DT be half of the above minimum and then compared our results in two ways. We checked the fourth-order Runge–Kutta method by comparing it with a simple forward Euler method. We checked the stability by halving the step size in time and noting that the results did not change.

In the simulations, we used periodic boundary conditions in both the spatial and the angular variable. This is the natural boundary condition for the angular variable. For the spatial variable, it is a simplification that allows us to ignore the effects of boundaries on the flux or the concentration of filaments. Essentially, since the region being simulated is a small part of the perimeter of a cell or other structure, this simplification is one way of 'isolating the region from the rest of the cell' and is simplest to implement numerically. The initial actin distribution was taken to be a 10% random deviation from the uniform steady-state situation in each case. The total concentration of actin was fixed at 15 μM and the α-actinin association rate, k_+, was fixed at 1 $\mu\mathrm{M}^{-1}\ \mathrm{s}^{-1}$.

8. RESULTS

The results of the simulations were put into the form shown in Figs 10–15. (A legend for the figures precedes the set of results.) In the results, each rectangle represents a one-dimensional corridor approximately 6 μ long, with actin filaments diffusing and interacting along the length of the corridor. The figures convey both the spatial and the angular distribution of the filaments. For this purpose, we have used a set of 32 'angular histograms' per frame (arrayed along the length of the region, at intervals corresponding to $6/32 = 0.1875$ μ). The length of the spokes on each of the wheels represents a local angular distribution of actin filaments. (For example, if the network is locally isotropic, showing no directional preference, the spokes are of equal length; if the actin is 'bundled' into preferred directions, some spokes are bigger than others: see figure legends for details.) The relative density of filaments is represented by the gray scale with light gray meaning low density and dark gray meaning high density.

In the sets of results, we show two time sequences. One consisting of Figs 10–12 shows a time-development of structures for a range of small filament lengths (0.4–1.0 μ) at times equivalent to 3, 8, and 15 min. The second sequence, Figs 13–15 shows the development of the structure when longer filaments (1.0–2.0 μ) are involved.

8.1. ***Effect of filament length.*** The results show the effect of filament length on the formation of spatio-angular patterns with two distinct regimes: where filaments are short enough that rotational diffusion dominates over translational diffusion (particularly for 0.4–0.6 μ), spatial clusters, rather than angular patterns form. This is shown by the lower frames in the time sequences, Figs 10–12. For this sequence, filaments of length $1, 0.8, 0.7, 0.6, 0.5, 0.4$ μ (top to bottom of

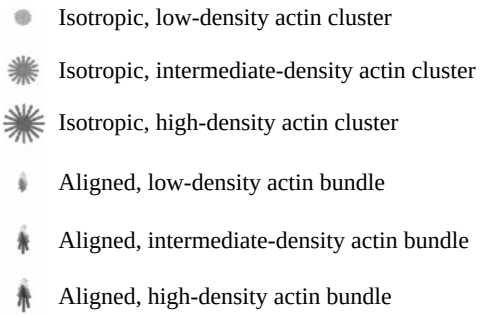

Figure 9. Legend for the angular histograms shown in the following figures.

figures) were used. It can be seen that 3 min into the dynamics, spatial clustering has begun to take place, with more closely spaced clusters in the lower filament length simulations (Fig. 10). By 8 min, the simulations of the longer filaments $(1, 0.8\ \mu)$ reveal a tendency of alignment into bundle-like structures, whereas in the other cases, clusters continue to grow and become more well-defined. By 15 min, $0.7\ \mu$ filaments which were previously dominated by clusters have also formed bundles, but smaller lengths have been frozen into clusters and will not align. The number of clusters (i.e. the wavenumber corresponding to the spatial periodicity) is greater for the smallest filament lengths. These frames reveal the tendency of smaller filaments to cluster first (and then possibly bundle).

In the second time sequence, Figs 13–15 filaments are longer than $1\ \mu$. (Unlike the previous figure, here filament lengths increase from the top to the bottom of the figure.) The corresponding magnitudes of the rotational and translational rates of diffusion in this regime are illustrated in Fig. 7. An intersection of the two graphs occurs at $1.6\ \mu$. For smaller lengths, the rotational diffusion rate is greater, and thus the tendency for alignment is depressed over the tendency for spatial segregation. Above $1.6\ \mu$, translational diffusion is faster, so there is fast mixing spatially, but the tendency for alignment is greater. Starting from an initially close to homogeneous and isotropic situation, by 5 min into the simulation, all frames reveal a tendency for alignment, with or without a superimposed spatial pattern. Bundles become more localized in the case where filaments are shorter, as expected.

8.2. ***Effect of viscosity.*** The viscosity of actin solutions *in vitro* are generally assumed to be close to that of water, namely 1 cP $=$ 0.01 P (Wachsstock *et al*., 1994), though this is an approximation that does not take into account the fact that the filaments themselves affect viscosity. In the cytoplasm, where there are a multitude of other particles, fibers, organelles, etc, viscosity is greater by orders of magnitude. (For example, Oster (1994) mentions a figure of 100–1000 P.) Viscosity, η_s influences both rotational and translational diffusion rates in the same way (it appears in the denominator of the expressions). A high value of the viscosity leads to a low value of the diffusion rates, and hence of the LHS

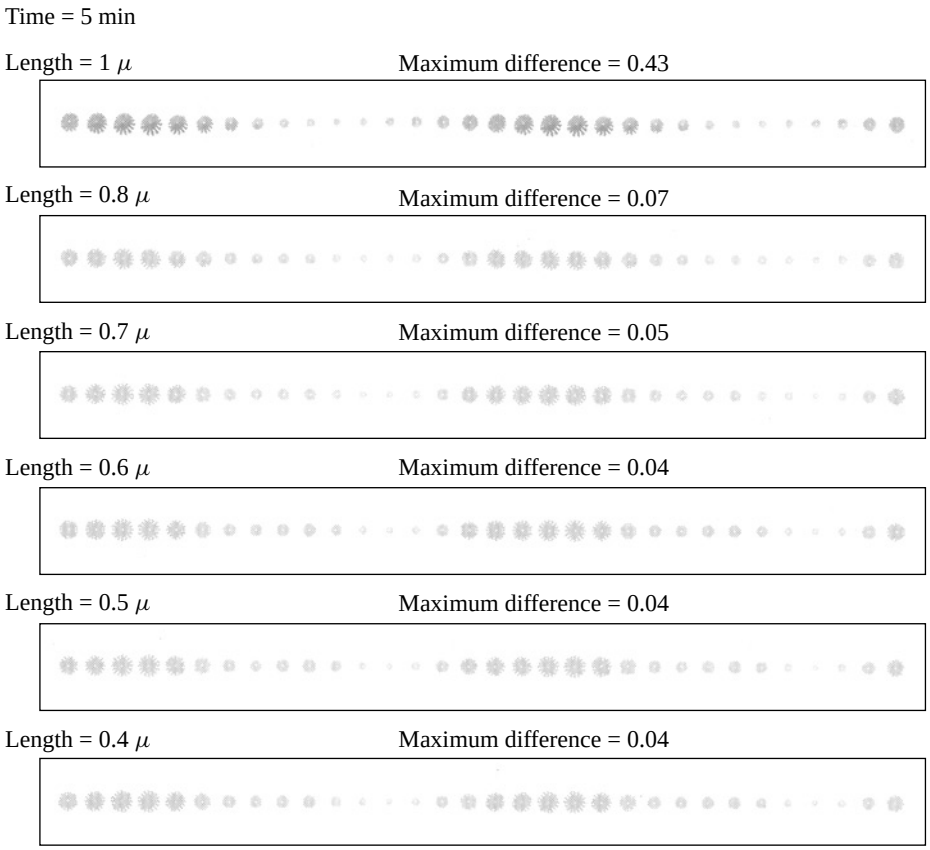

Figure 10. Spatio-angular distribution of actin filament density for filament lengths in the range 0.4–1 μ at time = 5 min. We show the local orientations and densities of actin in a region equivalent to a 6 μ long strip. The filaments retain a uniform angular distribution, but they tend to cluster in certain regions. See legend preceding this figure for an interpretation of the angular histograms used in this and the following figures.

of the instability condition. In other words, a high viscosity makes it more likely that instability at given wavenumbers would occur. All the simulations shown in Figs 10–15 were done with a value of viscosity much greater than that of water, i.e. 100 Poise.

When the viscosity is close to that of water, for an α-actinin concentration of 1 μM and small filament lengths (< 2 μ), no instability occurs, and the solution remains homogeneous and isotropic (both diffusion rates are far too rapid). For longer lengths (2–6 μ) we get alignment and no clustering. This is due to the effects of the length on the angular diffusion rate, μ_1 which is of order L^{-7}.

8.3. ***Effect of α-actinin concentration.*** We simulated both a high (10 μM) and a low (1 μM) concentration of α-actinin. The results of the case for high α-actinin have been described above. For the lower concentration, the time scale for pattern formation was much longer. Shorter filaments (2 μ) failed to cluster

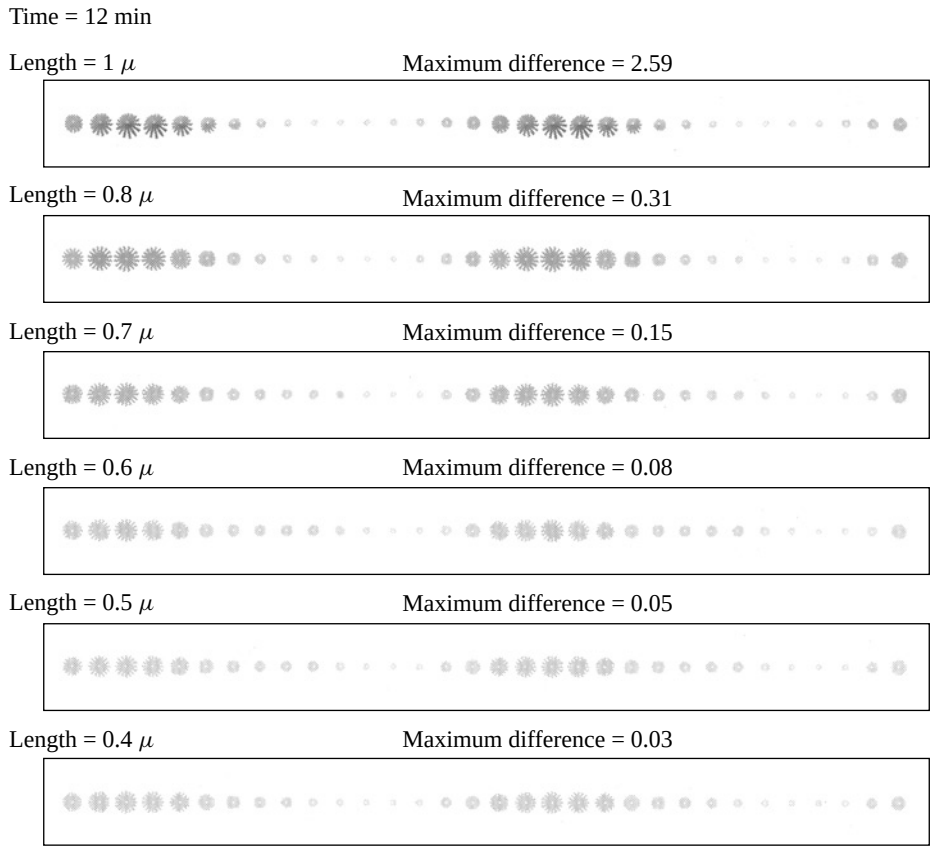

Figure 11. Same as Fig. 10 at time = 12 min. A slight tendency for alignment is seen in the longer filament length simulation (top). Shorter filaments (bottom) are beginning to aggregate and cluster somewhat, but they do not align.

or align even after 25 min. An intermediate size (3 μ) showed partial alignment which persisted. Only the longer (5 μ) filaments aligned completely everywhere.

8.4. ***Effect of the kernel.*** We found that only certain general properties of the kernels affect the final outcomes. For example, antiparallel and parallel kernels produced different results. Filaments were seen to align only in one direction in one case and to align in two directions, 180° apart from one another, in the other case. When the range of influence of a kernel is changed somewhat, the overall results are not greatly affected. Thus while the general properties of the kernel, such as its symmetry, greatly influence the final outcome, small changes in its shape have negligible effects, as noted previously by Mogilner and Edelstein-Keshet (1995).

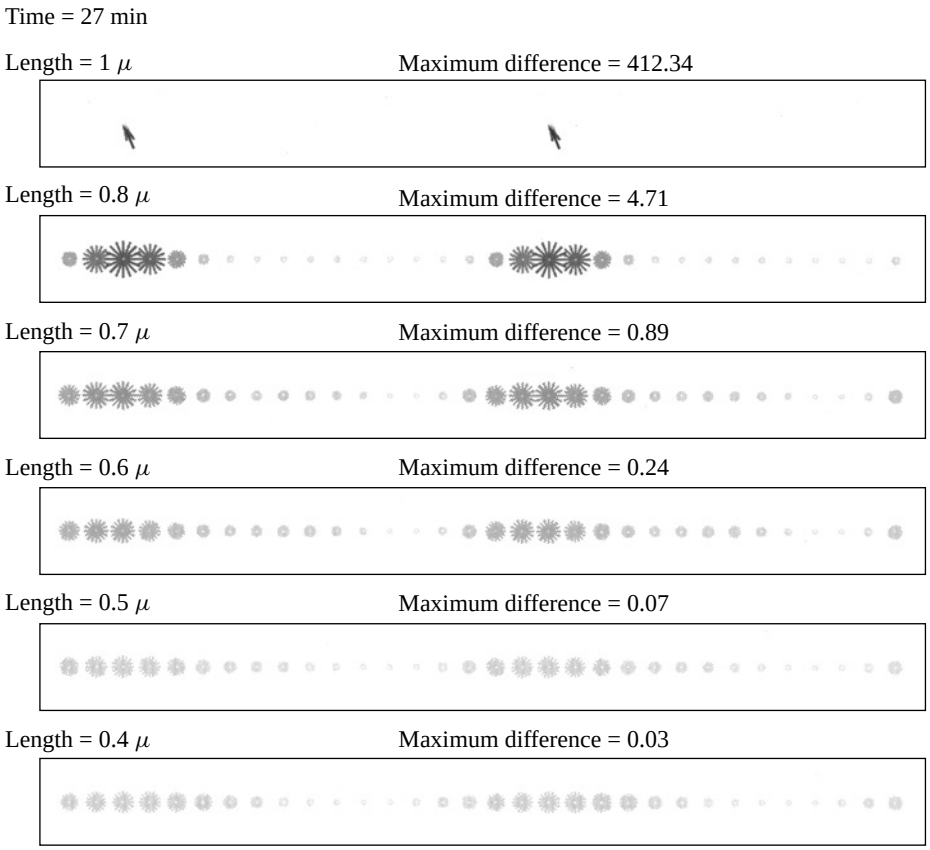

Figure 12. Same as Figs 10 and 11 at time = 27 min. The longest filaments (top) have aligned and formed 'bundles', while the shorter filaments (all others) only form clusters.

9. DISCUSSION

The results of the preliminary simulations have revealed an interesting effect of filament length on the types of patterns that tend to dominate. We have shown that under the conditions and parameter values which fit the biological scenario of actin filaments interacting via the crosslinker α-actinin, tendency to form clusters or bundles of actin depends in a sensitive way on the length of the filaments. These results can be understood partly in the context of the instability condition given by the inequality 4. We see that the ability to form patterns that have an angular component (represented by the wavenumber k_1), and those that have a spatial component (k_2) are mediated by rates of diffusion (rotational: μ_1, translational: μ_2). Manipulating filament lengths affects the relative magnitudes of these rates of diffusion, and thus determines for which values of the wavenumbers k_1, k_2 patterns can grow. When μ_1 is large, the patterns favored are those with $k_1 = 0$, whereas when μ_2 is large, patterns with $k_2 = 0$ are favored.

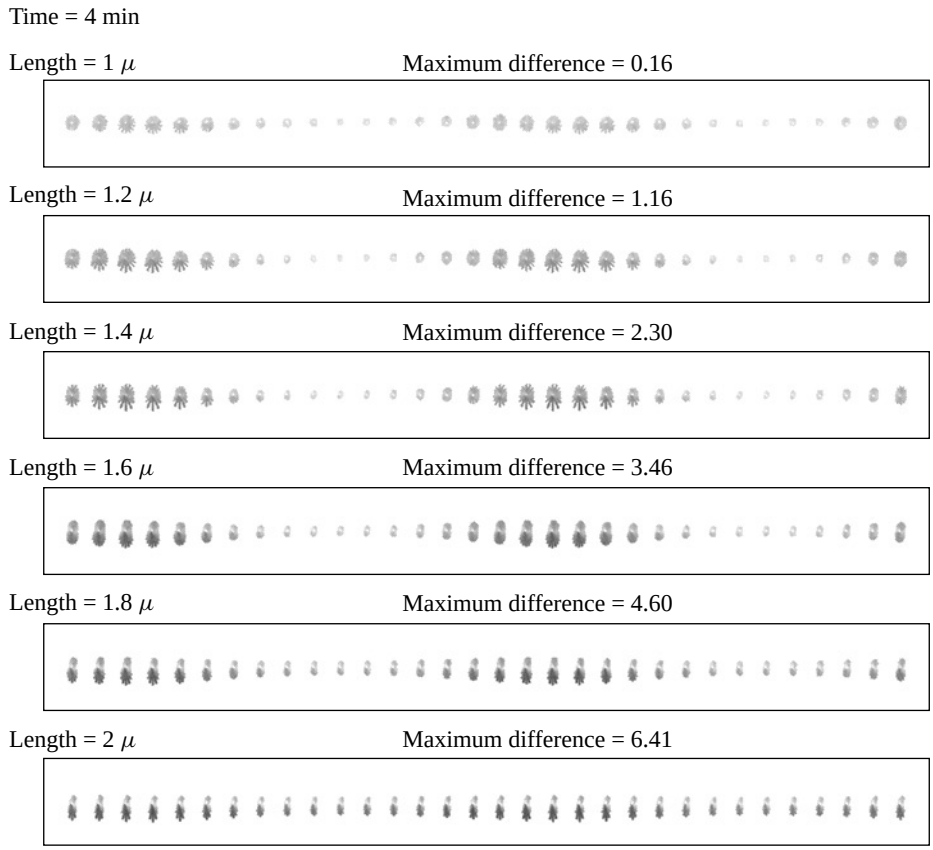

Figure 13. Spatio-angular distribution of actin filament density for filament lengths in the range 1.0–2.0 μ at time = 4 min. For longer filaments (bottom), angular alignment is favored over spatial clustering. Shorter filaments (top) prefer to cluster without alignment.

The length of actin filaments is controlled in the cell by the polymerization and depolymerization of actin monomers, and by fragmentation of filaments with agents such as gelsolin, fragmin and severin (Hartwig and Kwiatkowski, 1991). Recent modeling work describes how such processes influence both the distribution of filament lengths and the average length of the filaments (Edelstein-Keshet and Ermentrout, 1997; Ermentrout and Edelstein-Keshet, 1997). The preliminary results in this paper suggest the following intriguing hypothesis, namely that *by controlling processes that affect the length of its actin filaments, the cell can control transitions between random actin networks, actin clusters, and actin bundles.* Although the connection between filament length and filament order (e.g. alignment) has been mentioned in previous papers (Coppin and Leavis, 1992; Furukawa *et al*., 1993; Suzuki *et al*., 1991), we are unaware of previous models which have simulated the dynamics and lead to predictions based on biologically relevant parameter values.

The main attractive feature of the model is that it allows the nonlocal nature

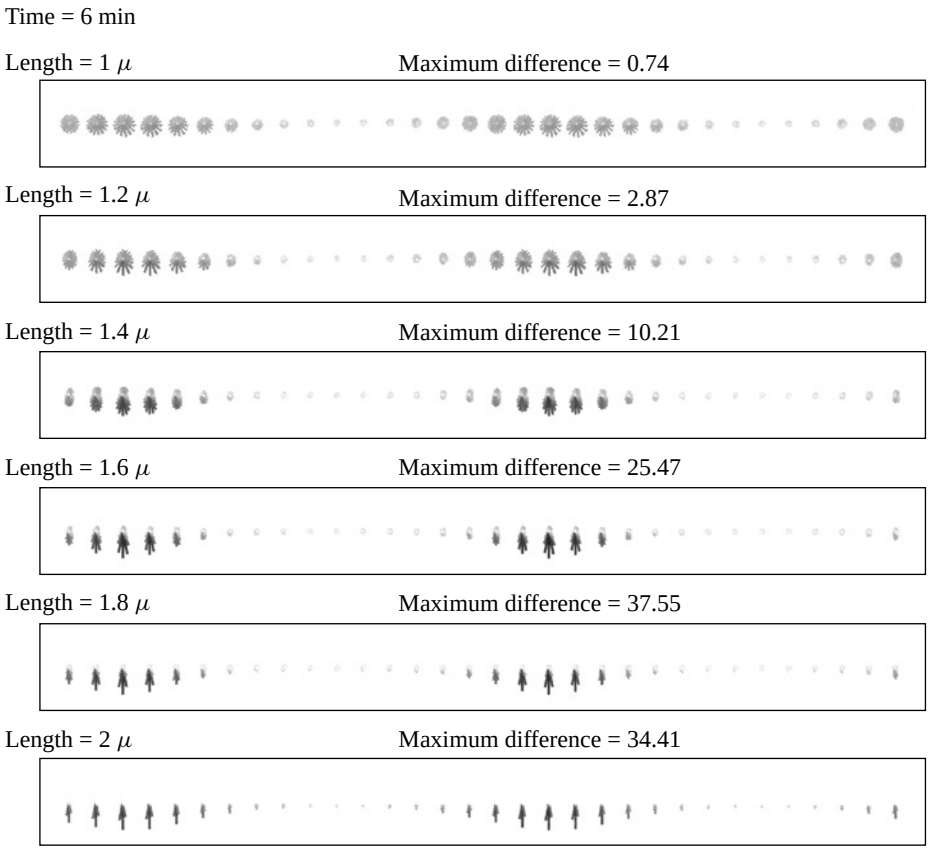

Figure 14. Same as Fig. 13 at time = 6 min. This figure shows that the degree of bundling depends on filament length.

of interactions of long rod-like polymers to be described. The basic idea may be relevant to other polymer interactions, where simple chemical-kinetic models fail to account for the spatially distributed nature of the interactions. However, while preliminary results give some interesting suggestions, it is necessary to point out several drawbacks and limitations of this model which mean that it must be viewed as a caricature, rather than a serious contender for a detailed molecular mechanism.

- In the model, actin filaments are viewed as stiff rods which have the same direction all along their length. It is known, however, that longer actin filaments (several μ long) are flexible, and thus this model would be inappropriate to describe these.
- The model assumes that a dominant effect shaping the cytoskeleton is the direct binding and unbinding of actin filaments (via crosslinkers), and neglects other processes such as *in situ* polymerization, motor-protein-induced rearrangements, etc.
- The model does not include mechanical forces that would tend to bend,

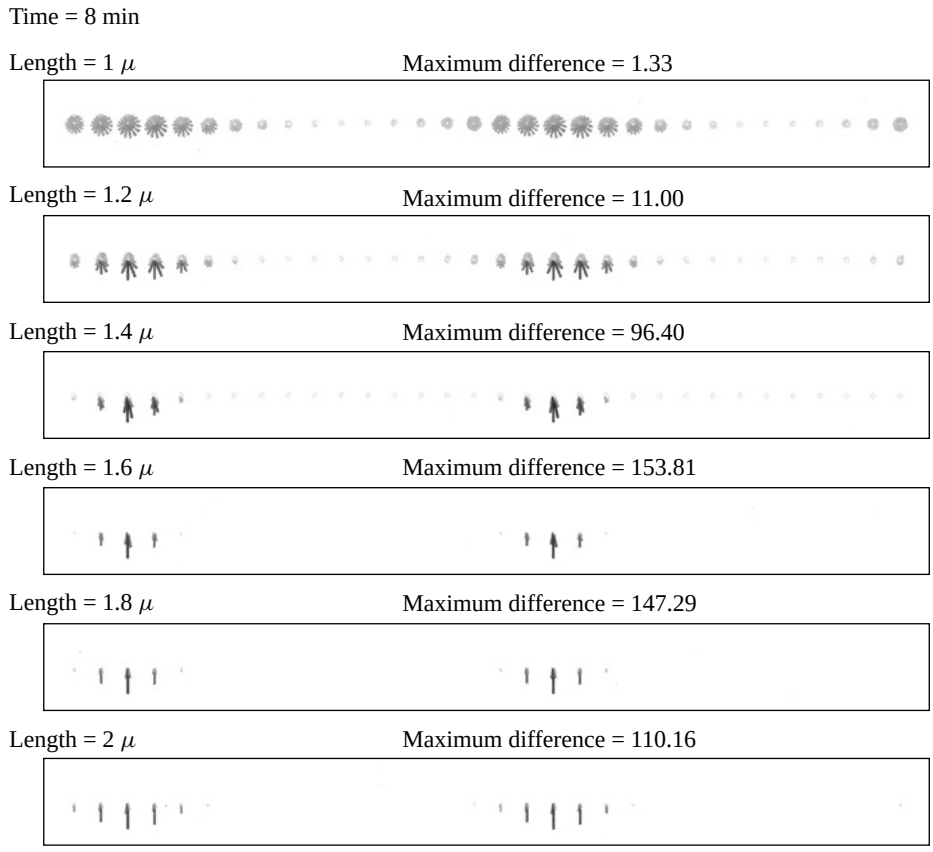

Figure 15. Same as Figs 13 and 14 at time = 8 min. All the simulations for these lengths lead to the formation of bundles. (See the simulation for filaments of length 1 μ shown in Fig. 12 for the final outcome.)

align, or hinder filament alignment. The effects of viscosity and other molecular clutter are included through the diffusion coefficients of the filaments, but not through the interaction terms.

- The effects of fluid convection are not included in the model. For cells in which cytoplasmic streaming is a dominant effect, this would be a shortcoming.
- The model assumes that the filaments can readily diffuse. This fits the *in vitro* experiments with actin concentration near 15 μM (the semi-dilute range). However, for *in vivo* actin concentrations closer to 100 μM (concentrated regime) diffusion of filaments is hampered. A different model is probably more appropriate for describing the higher actin concentration range.

Our simulations thus far have not produced the spatial mix of bundles, networks, and gels that characterize a region of the cell. This may stem from the simplistic model we are using, and may indicate defects that have to be corrected in more

realistic versions. For example, current failure to limit the build up of actin density at a given location is unrealistic, but can be amended in variants of the model. The fact that only one 'average' filament length is taken throughout may also be unrealistic when we try to extend the results to *in vivo* predictions. Finally, we are aware of the likelihood that the mechanisms for actin organization in real cells may be much more complicated than portrayed here. For example, the role of filament nucleation sites (e.g. at the cell membrane), the organization of polymerization inside the cell, mechanical effects due to motor proteins and fluid flows, and a variety of complicating effects that have been omitted here may eventually prove to be more important than the simple filament crosslinking dynamics that were described in this paper.

ACKNOWLEDGEMENTS

The authors would like to thank Alex Mogilner for discussions at the early stages of this work. This research is supported by an NSERC Operating Grant from GSC 21 to Leah Edelstein-Keshet. Work in collaboration with Edith Geigant and Wolfgang Alt in the initial stages of this research were also supported by a NATO grant to Dr Alt and Dr Edelstein-Keshet.

APPENDIX

A.1. Further mathematical details about the model. The homogeneous steady states of the model satisfy

$$\beta_1 \bar{F}^2 + \beta_2 \bar{F}\bar{N} = \gamma \bar{N}. \tag{26}$$

We let $M = \bar{N} + \bar{F}$. If $\beta_1 = \beta_2 = \beta$, then

$$\bar{F} = \frac{\gamma M}{\beta M + \gamma}, \tag{27a}$$

$$\bar{N} = \frac{\beta M^2}{\beta M + \gamma}. \tag{27b}$$

The equations can be written in dimensionless form:

$$N_t(x,\theta,t) = FK * F + \beta' NK * F - \gamma' N\,, \tag{28a}$$

$$F_t(x,\theta,t) = \epsilon_1 \Delta_\theta F + \epsilon_2 \Delta_x F - FK * F - \beta' FK * N + \gamma' N\,. \tag{28b}$$

where:

$$\gamma' = \frac{\gamma}{\beta_1 M}, \epsilon_1 = \frac{\mu_1}{\beta_1 M}, \epsilon_2 = \frac{\mu_2}{\beta_1 M L^2}, \beta' = \frac{\beta_2}{\beta_1}, \tag{29}$$

with L a (spatial) length scale, (in this case the average length of the filaments). The variables N and F are scaled in terms of M. (The definition of the dimensionless parameters given in Mogilner and Edelstein-Keshet (1996) was erroneous.)

When $\beta_1 = \beta_2 = \beta$, the condition for instability, in terms of the dimensionless parameters is:

$$\epsilon_1 k_1^2 + \epsilon_2 k_2^2 < \left(\frac{1}{\gamma'}\right)^2 \hat{K}(1 - \hat{K}). \tag{30}$$

More generally, when $\beta_1 \neq \beta_2$, we define $\tilde{M} = \bar{F} + (\beta_2/\beta_1)\bar{N}$. The condition for instability is then as given by equation (4).

A.2. Units and conversion factors. Concentrations are specified in the literature either as units of mass per unit volume, for example as mg ml^{-1} or as μM. A typical actin concentration *in vitro* is 1 mg ml^{-1}. The model is based on interactions of whole filaments, and thus keeps track of the number of filaments per unit volume. To convert from one set of units to the other we note that 1 Mole contains 6.02×10^{23} molecules (Avogadro's number). 1 M = 1 M per liter. (Further 1 ml = 1 $\text{cm}^3 = 10^{12}$ μ^3). Thus

$$1 \text{ M} = 6.02 \times 10^{23} \text{molecules per liter}, \tag{31}$$

$$1\ \mu\text{M actin} = 6.02 \times 10^{17} \text{ monomers per liter} = 6.02 \times 10^{14} \text{ monomers per ml} = 602 \text{ monomers per } \mu^3. \tag{32}$$

The molecular weight of an actin monomer is 46,000 daltons (1 dalton is the mass of one hydrogen atom = 1.67×10^{-24} gm). Thus, the mass of an actin monomer is 7.7×10^{-17} mg.

$$1 \text{ mg actin} = 1.3 \times 10^{16} \text{ monomers}, \tag{33}$$

$$1\ \mu \text{ length actin filament} = 370 \text{ monomers}. \tag{34}$$

A concentration of 1 μM of actin monomers can produce a total length of 602/370 = 1.63 μ in a volume of 1 μ^3. Therefore, if the total concentration of actin in filaments and the average length of a filament L is given, then the number of filaments of length L per unit volume, ν is

$$\nu = \left(\frac{\text{number of filaments}}{\mu^3}\right) \tag{35}$$

$$\nu = \begin{pmatrix}\text{mass actin per}\\ \text{unit volume}\end{pmatrix} \times \begin{pmatrix}\text{number of}\\ \text{monomers}\\ \text{per unit}\\ \text{mass}\end{pmatrix} \times \begin{pmatrix}\text{length}\\ \text{per}\\ \text{monomer}\end{pmatrix} \times \left(\frac{1}{\text{filament length}}\right) \tag{36}$$

or simply

$$\nu = \left(\frac{1 \text{ mg}}{1 \text{ ml}}\right)\left(\frac{1 \text{ ml}}{10^{12}\mu^3}\right)\left(\frac{1.3 \times 10^{16} \text{ monomers}}{1 \text{ mg}}\right)\left(\frac{1\ \mu}{370 \text{ monomers}}\right)\left(\frac{1}{L}\right). \tag{37}$$

α-actinin is a dimer, consisting of two identical subunits (Meyer and Aebi, 1990) with a total molecular weight 200 000 daltons (100 K daltons per subunit). A conversion from mass concentration to number concentration is

$$1 \text{ mg of } \alpha\text{-actinin} = 3 \times 10^{15} \text{ molecules of } \alpha\text{-actinin}. \tag{38}$$

Several other parameters and constants must be converted. To convert k_+ (which is generally given in units of $\mu\text{M}^{-1}\ \text{s}^{-1}$) to units used here, note that.

$$1\ \mu\text{M}^{-1}s^{-1} = 3.3 \times 10^{-3}\mu^3 \text{ per } \alpha\text{-actinin dimer } \text{s}^{-1}. \tag{39}$$

REFERENCES

Alberts, B, D. Bray, J. Lewis, M. Raff, M. Roberts and J. D. Watson (1989). *Molecular Biology of the Cell*. New York: Garland.

Bray, D. (1992). *Cell Movements*. New York: Garland.

Burridge K. and J. R. Feramisco (1981). Non-muscle α-actinins are Calcium-sensitive Actin-binding Proteins. *Nature* **294**, 565–567.

Civelekoglu, G. and L. Edelstein-Keshet (1994). Models for the formation of actin structures. *Bull. Math. Biol.* **56**, 587–616.

Colombo, R., I. DalleDonne and A. Milzani (1993) α-Actinin Increases Actin Filament End Concentration by Inhibiting Annealing. *J. Mol. Biol.* **230**, 1151–1158.

Coppin, C. M. and P. Leavis (1992). Quantitation of liquid-crystaline ordering in F-actin solutions. *Biophys J.* **63**, 794-807.

Doi, M. and S. F. Edwards (1986). *The Theory of Polymer Dynamics*, Oxford: Clarendon Press.

Edelstein-Keshet, L. and G. B. Ermentrout (1990). Models for contact-mediated pattern formation: cells that form parallel arrays. *J. Math. Biol.* **29**, 33-58.

Edelstein-Keshet, L. and G. B. Ermentrout (1998). Models for the length distribution of actin filaments: I Simple polymerization and fragmentation acting alone. *Bull. Math. Biol.*, in press.

Ermentrout, G. B. and L. Edelstein-Keshet (1998). Models for the length distribution of actin filaments: II: Polymerization and Fragmentation by Gelsolin acting together. *Bull. Math. Biol.*, in press.

Furukawa, R., R. Kundra and M. Fechheimer (1993). Formation of liquid crystals from actin filaments. *Biochemistry* **32**, 12346–12352.

Geigant, E., K. Ladizhansky and A. Mogilner (1997). Integro-differential model for orientational distribution of F-actin in cells. *SIAM J. Appl. Math.*, in press.

Geigant, E. and M. Stoll, (1996). A non-local model for alignment of oriented particles. *Research Summary*. Bonn University.

Giuliano, K. A. and D. L. Taylor (1995). Measurement and manipulation of cytoskeletal dynamics in living cells. *Current Opinion Cell Biol.* **7**, 4–12.

Gorlin, J. B., R. Yamin, S. Eagen, M. Stewart, T. P. Stossel, D. J. Kwiatkowski and J. H. Hartwig (1990). Human endothelial actin-binding protein (ABP-280, nonmuscle filamin): a molecular leaf spring. *J. Cell. Biol.* **111**, 1089–1105.

Hartwig, J. H. and D. J. Kwiatkowski (1991). Actin binding proteins. *Current Opinion Cell Biol.* **3**, 87–97.

Hartwig, J. H., J. Tyler and T. P. Stossel (1980). Actin-binding protein promotes the bipolar and perpendicular branching of actin filaments. *J. Cell. Biol.* **87**, 841–848.

Jacquez J. A. (1972). *Compartmental Analysis in Biology and Medicine*, Amsterdam: Elsevier.

Janmey, P. A., S. Hvidt, J. Käs, D. Lerche, A. Maggs, E. Sackmann, M. Schliwa and T. P. Stossel (1994). The Mechanical Properties of Actin Gels. *J. Biol. Chem.* **269**, 32503–32513.

Janmey, P. A., J. Peetermans, K. S. Zaner, T. P. Stossel and T. Tanaka (1986). Structure and Mobility of actin filaments as measured by quasielectric light scattering, viscometry and electron microscopy. *J. Biol. Chem.* **261**, 8357–8362.

Janson, L. W. and D. L. Taylor (1994). Actin-crosslinking protein regulation of filament movement in motility assays: a theoretical model. *Biophys. J.* **67**, 973–982.

Jockusch, B. M. and G. Isenberg (1981). Interaction of α-Actinin and Vinculin with Actin: Opposite effects on Filament Network Formation. *Proc. Nat. Acad. Sci. USA*. **78**, 3005–3009.

Ladizhansky, K. (1994). *Distribution of generalized aspect with applications to actin fibers and social interactions, Technical Report*, MSc thesis Weizmann Institute of Science, Rehovot, Israel.

Luby–Phelps, K. (1994). Physical Properites of Cytoplasm. *Current Opinion Cell Biol.* **6**, 3–9.

Lumsden, C. J. and P. A. Dufort (1993). Cellular Automaton Model of the Actin Cytoskeleton. *Cell Motil. Cytoskel.* **25**, 87–104.

McGough, A. (1997). Structural Studies of Gelsolin: Actin Interactions, Baylor College of Medicine, Houston, http://dali.bcm.tmc.edu/ amy/Gelsolin.html

Maciver, S. K., D. H. Wachsstock, W. H. Schwarz and T. D. Pollard (1991). The actin filament severing protein acotophorin promotes the formation of rigid bundles of actin filaments crosslinked with α-actinin. *J. Cell Biol.* **115**, 1621–1628.

Meyer, R. K. and U. Aebi (1990). Bundling of actin filaments by α-actinin depends on its molecular length. *J. Cell Biol.* **110**, 2013–2024.

Mogilner, A. and L. Edelstein-Keshet (1995). Selecting a common direction I. How orientational order can arise from simple contact responses between interacting cells. *J. Math. Biol.* **33**, 619–660.

Mogilner, A. and L. Edelstein-Keshet (1996). Spatio-angular order in populations of self-aligning objects: formation of oriented patches. *Physica* **D89**, 346–367.

Niederman, R. R., P. C. Amrein and J. Hartwig (1983). Three-dimensional structure of actin filaments and of an actin gel made with actin-binding protein. *J. Cell. Biol.* **96**, 1400–1413.

Oster, G. F. (1994). *Biophysics of Cell Motility*, Lecture Notes, University of California Berkeley.

Otto, J. J. (1994). Actin-bundling proteins. *Current Opinion Cell Biol.* **6**, 105–109.

Parfenov, V. N., D. S. Davis, G. N. Pochukalina, C. E. Sample, E. A. Bugaeva and K. G. Murti (1995). Nuclear actin filaments and their topological changes in frog oocytes.

Exp. Cell Res. **217**, 385–394.
Suzuki, A., T. Maeda and T. Ito (1991). Formation of liquid crystalline phase of actin filament solutions and its dependence on filament length as studied by optical birefringence. *Biophys. J.* **59**, 25-30.
Taylor, K. A. and D. W. Taylor (1994). Formation of two-dimensional complexes of F-Actin and crosslinking proteins on Lipid monolayers: demonstration of unipolar α-actinin–F-actin crosslinking. *Biophys. J.* **67**, 1976–1983.
Wachsstock, D. H., W. H. Schwarz and T. D. Pollard (1993). Affinity of α–Actinin for actin determines the structure and mechanical properties of actin filament gels. *Biophys. J.*, **65**, 205–214.
Wachsstock, D. H., W. H. Schwarz and T. D. Pollard (1994). Cross–linker dynamics determine the mechanical properties of actin gels. *Biophys. J.* **66**, 801–809.
Zaner, K. S. (1995). Physics of actin networks. I. Rheology of semi-dilute F-Actin. *Biophys. J.* **68**, 1019–1026.

Received 24 April 1997 and accepted 16 September 1997